RENAL FAILURE
2025, VOL. 47, NO. 1, 2480749
https://doi.org/10.1080/0886022X.2025.2480749

Taylor & Francis
Taylor & Francis Group

LABORATORY STUDY



# Fecal microbiota transplantation modulates myeloid-derived suppressor cells and attenuates renal fibrosis in a murine model

Yajie Wang[a,b,c], Yuye Chen[a], Zihao Xiao[a], Yuanhui Shi[a], Cong Fu[d] and Yuhan Cao[a]

[a]Department of Nephrology, The First Affiliated Hospital of Wannan Medical College, Wuhu, Anhui, China; [b]Anesthesia Laboratory and Training Center of Wannan Medical College, Wuhu, Anhui, China; [c]Key Laboratory of Non-coding RNA Transformation Research of Anhui Higher Education Institution (Wannan Medical College), Wuhu, Anhui, China; [d]Department of Cardiology, The First Affiliated Hospital of Wannan Medical College, Wuhu, Anhui, China

**ABSTRACT**

**Background:** Renal fibrosis is a hallmark of progressive chronic kidney disease (CKD), with emerging evidence linking gut microbiota dysbiosis to disease progression. Myeloid-derived suppressor cells (MDSCs) have demonstrated renoprotective effects, yet the impact of fecal microbiota transplantation (FMT) on MDSC-mediated modulation of renal fibrosis remains unclear.
**Methods:** C57BL/6J mice underwent unilateral ureteral obstruction (UUO) to induce renal fibrosis, followed by FMT administration *via* gavage. Flow cytometry was used to quantify granulocytic (G-MDSCs) and monocytic (M-MDSCs) MDSC populations in peripheral blood, kidney, and spleen. To elucidate the role of MDSCs in FMT-mediated effects, MDSCs were depleted or adoptively transferred *in vivo*. Renal fibrosis severity and inflammatory cytokine expression were subsequently analyzed.
**Results:** FMT altered MDSC distribution, increasing M-MDSC accumulation in the blood and kidney. This was associated with downregulation of proinflammatory cytokines and attenuation of renal fibrosis. Adoptive MDSC transfer similarly produced anti-inflammatory and antifibrotic effects, reinforcing their therapeutic role in FMT-mediated renal protection.
**Conclusions:** FMT enhances M-MDSC-mediated immunomodulation, reducing inflammation and renal fibrosis in UUO-induced CKD. These findings suggest a potential therapeutic strategy targeting the gut-kidney axis in CKD management.

**ARTICLE HISTORY**
Received 7 December 2024
Revised 7 March 2025
Accepted 9 March 2025

**KEYWORDS**
Chronic kidney disease; fecal microbiota transplantation; gut microbiota; myeloid-derived suppressor cells; renal fibrosis; inflammation

## Introduction

Chronic kidney disease (CKD) affects patient health and quality of life in a variety of ways and has a high mortality rate [1]. Renal fibrosis is the buildup of scars within the parenchyma, and it represents the common final pathway of nearly all chronic and progressive nephropathies [2]. It is difficult to ameliorate or reverse the progression of renal fibrosis. Therefore, there is still an urgent need to explore feasible ways to address this challenge.

Microbiome homeostasis has been described as an important contributor to human health [3]. It constantly communicates with vital organ systems of the host, forming the gastrointestinal-renal axis, brain-gut axis, and gut-renal axis [4,5]. Recent analyses have shown that the gut microbiome also influences the dynamics of immune cells [6]. This communication contributes to the homeostasis and health of the host. However, once the homeostasis was disrupted, the composition of the gut microbiota would also changed markedly. A previous study, utilizing 16S ribosomal DNA (rDNA) sequencing and metabolomics methods, discovered a decrease in the genera of gut microbiota producing short-chain fatty acids in renal fibrosis animals induced by UUO [7]. In W. Zhou's study, we found that the abundance of *Bacteroides fragilis* (*B. fragilis*) in the fecal samples of UUO mice was significantly decreased [8]. The role of the gut microbiota in CKD has been emphasized. There is a two-way regulatory relationship between the gut microbiota and CKD [9]. On the one hand, CKD results in altered gut microbiota and metabolites derived from the gut microbiota. On the other hand, decreased production of molecules related to the anti-inflammatory and antifibrotic effects in the microbiome promotes the toxic uremic environment in CKD [10,11]. Fecal microbiota transplantation (FMT) involves the infusion of stool from a healthy donor into the gastrointestinal (GI) tract of a recipient patient for

**CONTACT** Yuhan Cao caoyuhan@wnmc.edu.cn Department of Nephrology, The First Affiliated Hospital of Wannan Medical College, 92# West Zhe Shan Road, Wuhu, Anhui, China; Cong Fu fucong@wnmc.edu.cn Department of Cardiology, The First Affiliated Hospital of Wannan Medical College, 92# West Zhe Shan Road, Wuhu, Anhui, China.

Supplemental data for this article can be accessed online at https://doi.org/10.1080/0886022X.2025.2480749.

therapeutic purposes. As a valid microbiome-based invention, FMT is a highly effective treatment for recurrent *Clostridium difficile* infection (CDI) [12]. Moreover, a study has shown that FMT limits the accumulation of uremic toxins through beneficial effects on gut microbiota diversity [13]. However, research on the therapeutic potential of FMT in renal inflammation and fibrosis remains limited.

Myeloid-derived suppressor cells (MDSCs) are a heterogeneous population of immature myeloid cells consisting of myeloid progenitor cells and precursors of macrophages, granulocytes and dendritic cells (DCs) with potent immunosuppressive activity [14]. MDSCs express Gr-1 and CD11b in mice. Based on their phenotypic and morphological features, MDSCs are divided into two major subsets: granulocytic-MDSCs (G-MDSCs) and monocytic-MDSCs (M-MDSCs) [15]. In mice, G-MDSCs are defined as $CD11b^{+}Ly6G^{+}Ly6C^{low,}$ and M-MDSCs are defined as $CD11b^{+}Ly6G^{-}Ly6C^{high}$ [15]. The adoptive transfer of MDSCs has demonstrated efficacy in the treatment of acute kidney injury and chronic renal failure [16,17]. A recent study revealed that the recruitment of MDSCs can also be influenced by the gut microbiota [18]. However, there is a lack of studies on how the microbiota affects MDSCs in renal fibrosis. Therefore, this study explored how FMT alters the subsets of MDSCs in mice with renal fibrosis, thereby affecting the production of inflammatory factors.

## Materials and methods

### Animals

Six-week-old C57BL/6J mice weighing 20–25 g were obtained from GemPharmatech Co., Ltd. (Nanjing, China) and bred in a specific pathogen-free (SPF) grade animal room. Mice were allowed a one-week period of acclimatization with free access to food and water and were housed under a 12 h light/dark cycle. Mice were used according to the guidelines of the Animal Ethics Committee of Wannan Medical College (LLSC-2022-142).

### Fecal microbiota transplantation (FMT)

We chose oral fecal gavage as described previously [19,20]. Before FMT treatment, the mice were given three antibiotics (1.25 mg/L vancomycin, 2.5 mg/L penicillin, and 2.5 mg/L metronidazole) by gavage at 0.2 mL/day for 3 days to remove native gut microbes [21]. For FMT experiments, 200 mg of stool was collected daily from the control group, resuspended in 3 mL of PBS, and then homogenized for 3 min before large particles were removed by filtration. Nine milliliters of PBS was added to the filtrate, which was subsequently centrifuged at 3000 ×*g* for 15 min. Finally, the supernatant was collected for transplantation. Mice were intragastrically administered 0.2 mL of fresh fecal solution once daily for 7 days.

### Grouping and animal model establishment

The mice were randomly divided into seven groups ($n = 6$). (1) In the control group, the mice did not undergo any surgery. (2) In the unilateral ureter obstruction (UUO) group, mice underwent UUO. (3) In the FMT treatment group (UUO+FMT), UUO was performed before FMT treatment. (4) In the Splenectomy group (UUO+FMT+Splenectomy), splenectomy and UUO were performed before FMT treatment. (5) In the Gemcitabine group (UUO+FMT+GEM), mice underwent UUO, and then gemcitabine (100 mg/kg; Shanghai Macklin Biochemical Co., Ltd., China) was intraperitoneally administered to the mice during FMT treatment. (6) In the MDSC adoptive transfer group (MDSCs transfer), MDSCs from the peripheral blood in the UUO+FMT group were separated by a magnetic column and then infused through the angular vein into mice that had undergone UUO and splenectomy. (7) In the control cell adoptive transfer group (Negative transfer), the negative control cells that were not adsorbed by the magnetic column after sorting the MDSCs were infused into mice. For UUO experiments, after anesthetizing the mice, the left kidney was exposed through a midline incision. The left ureter was isolated and ligated at two points with nonabsorbable 5–0 silk sutures and then cut between the ligatures. Splenectomy was performed as previously described [22]. After ligation of the relevant vessels, the spleen was removed to separate it from the stomach. Then, the midline fascial defect and skin were sutured.

### Flow cytometric analyses

Mice were sacrificed by spinal cord dislocation 14 days after UUO surgery. The spleens and kidneys were ground in PBS containing 1% bovine serum albumin (BSA). Red blood cells in peripheral blood were depleted with red blood cell lysis buffer (Beyotime, China). The cell suspension was then filtered through a 40 μm cell strainer (Biologix, USA) to remove aggregates and debris. The cells were stained with fluorophore-conjugated antibodies, including PE-conjugated anti-mouse/human CD11b (BioLegend, USA), FITC-conjugated anti-mouse Ly-6C/Ly-6G (Gr-1) (BioLegend, USA), APC-conjugated anti-mouse Ly-6C (BioLegend, USA), and FITC-conjugated anti-mouse Ly-6G (BioLegend, USA), for 30 min at room temperature in staining buffer. The data were acquired on a BD FACSVerse flow cytometer (BD Biosciences, USA) and analyzed with FlowJo X.

### Isolation and adoptive transfer of MDSCs

Mononuclear cells in peripheral blood were separated with lymphocyte separation medium (Biosharp, China) and red blood cell lysis buffer (Beyotime, China). After centrifugation (300 × g for 10 min), the cells were resuspended at $10^8$ cells/mL in buffer solution. MDSCs were isolated by using a mouse MDSC isolation kit (Miltenyi Biotec, Germany) according to the manufacturer's protocol. Specifically, $Gr\text{-}1^{high}Ly\text{-}6G^{+}$ cells were indirectly magnetically labeled with anti-Ly-6G-Biotin and anti-Biotin MicroBeads and then magnetically separated to obtain pre-enriched $Gr\text{-}1^{dim}Ly\text{-}6G^{-}$ cells (flow-through fraction) and enriched $Gr\text{-}1^{high}Ly6G^{+}$ cells (positive selection fraction). Subsequently, indirect magnetic labeling of pre-enriched $Gr\text{-}1^{dim}Ly\text{-}6G^{-}$ cells was performed using anti-Gr-1-biotin and

streptavidin microbeads, and then magnetic separation was performed to obtain enriched Gr-1$^{dim}$Ly- 6G$^{-}$ cells. MDSCs were derived from a mixture of Gr-1$^{high}$Ly6G$^{+}$ cells and Gr-1$^{dim}$Ly- 6G$^{-}$ cells. FACS was used to evaluate the separation efficiency of the isolated MDSCs. The purified MDSCs ($2\times10^{6}$) and the negative control cells were adoptively transferred to mice *via* the angular vein every 4 days.

### Histopathology

Renal tissues from the mice were fixed in 4% paraformaldehyde for 24 h immediately after sacrifice, embedded in paraffin, and sliced into 3 µm thick sections. After deparaffinizing and rehydrating, hematoxylin–eosin (HE) staining kits were used for HE staining (Solarbio, China). Masson's trichrome stain kits were used for Masson staining (Solarbio, China). The stained sections were examined using an optical microscope in a blinded manner. ImageJ was used to determine the positive area of Masson's trichrome staining (blue).

### Immunofluorescence staining

To detect the expression of TNF-α and IL-10 in renal tissue, paraffin-embedded renal tissue sections (3 µm thick) were stained with a TNF-α rabbit polyclonal antibody (Beyotime, China) and an IL-10 rabbit polyclonal antibody (Beyotime, China) at 4 °C overnight. Then, the sections were stained with an Alexa Fluor 647-labeled goat anti-rabbit secondary antibody (Beyotime, China) for two hours at room temperature. Nuclei were stained with DAPI (Beyotime, China) for ten minutes. Confocal imaging was performed using a Leica TCS SP8 confocal microscope (Leica, Germany).

### qRT–PCR

Total RNA was collected from kidney tissues using TRIzol reagent. First-strand cDNA was synthesized using a PrimeScript™ RT reagent kit (TAKARA, Japan) with gDNA Eraser according to the manufacturer's instructions. Then, PCR was performed using a TB Green Premix Ex Taq Kit (TAKARA, Japan) according to the manufacturer's protocol. CD11b (Forward: CCATGACCTTCCAAGAGAATGC, Reverse: ACCGGCTTGTGCTGTAGTC), Gr-1 (Forward: TCATCCTTCTTGTGGT CCTA, Reverse: AAGGGGCAGGTAGTTGTG), IL-10 (Forward: GGTTG TCGTCTCATTCTGAAAGA, Reverse: GGTAGAGGACCCAAGTTCGTTAA GA), TNF-α (Forward: GCCCACATCAGCTATTGTTCGT, Reverse: CAGGAATAGCAACAGGCATGGT), and β-actin (Forward: GTCGT ACCAC AGGCA TTGTG ATGG, Reverse: GCAAT GCCTG GGTAC ATGGT GG) primers were used. Relative expression levels were normalized to β-actin expression and calculated according to the standard $2^{-\Delta\Delta Ct}$ method.

### Western blot

For Western blot analysis, protein was extracted from mouse kidney tissue using phenylmethanesulfonyl fluoride (PMSF) and radioimmunoprecipitation assay (RIPA) lysis buffer (Beyotime, China). Protein concentrations were measured using a BCA assay kit (Beyotime, China). Whole extracts were separated by 12% sodium dodecyl sulfate–polyacrylamide gel electrophoresis (SDS–PAGE). After being transferred to a polyvinylidene difluoride (PVDF) membrane, the membrane was incubated with diluted primary antibodies, including a TNF-α rabbit polyclonal antibody (Beyotime, China), an IL-10 rabbit polyclonal antibody (Beyotime, China), and a GAPDH antibody (Biosharp, China). Then, the membranes were incubated with the corresponding secondary antibodies (Biosharp, China). The band intensity was analyzed using ImageJ software and normalized to the band intensity of GAPDH.

### Statistical analysis

SPSS software (SAS Institute Inc., USA) was used for data analysis. Quantitative data are presented as the mean ± SD, and the data were statistically evaluated using Student's t-tests and one-way ANOVA. A value of $p<0.05$ was considered to indicate statistical significance.

## Results

### FMT regulated MDSC mobilization after UUO

Mouse samples were harvested 14 days after surgery (Figure 1(A)). In renal tissue, qRT–PCR revealed that Gr-1 expression was increased in the UUO+FMT group compared to the UUO group, and CD11b expression tended to decrease, but the difference was not statistically significant (Figure 1(B)). We found that the G-MDSC proportions in the peripheral blood and kidney were significantly greater in the UUO group than in the control group (Figure 1(C)). However, compared with those in the UUO group, the percentages of G-MDSCs in the peripheral blood and kidneys in the UUO+FMT group were decreased. Moreover, the percentage of M-MDSCs was significantly increased (Figure 1(C)). These results confirmed that FMT treatment resulted in altered percentages of G-MDSCs and M-MDSCs in UUO model mice. More M-MDSCs accumulated in the circulation and kidney.

### FMT protected against UUO injury

We investigated the efficacy of FMT treatment on renal injury. HE staining revealed inflammatory cell infiltration and tubular deformation in the renal tissues of UUO model mice compared with those of control mice, while FMT intervention significantly alleviated renal injury (Figure 2(A)). Masson's trichrome staining revealed obvious interstitial fibrosis in UUO model mice, but this effect was attenuated by FMT (Figure 2(A,B)). We then examined the proinflammatory cytokine TNF-α and the anti-inflammatory cytokine IL-10 to evaluate renal inflammation. qRT–PCR and Western blot analysis revealed low TNF–α and IL–10 expression in the control group (Figure 2(C,D)). We found that TNF-α protein expression was significantly upregulated 14 days after UUO,

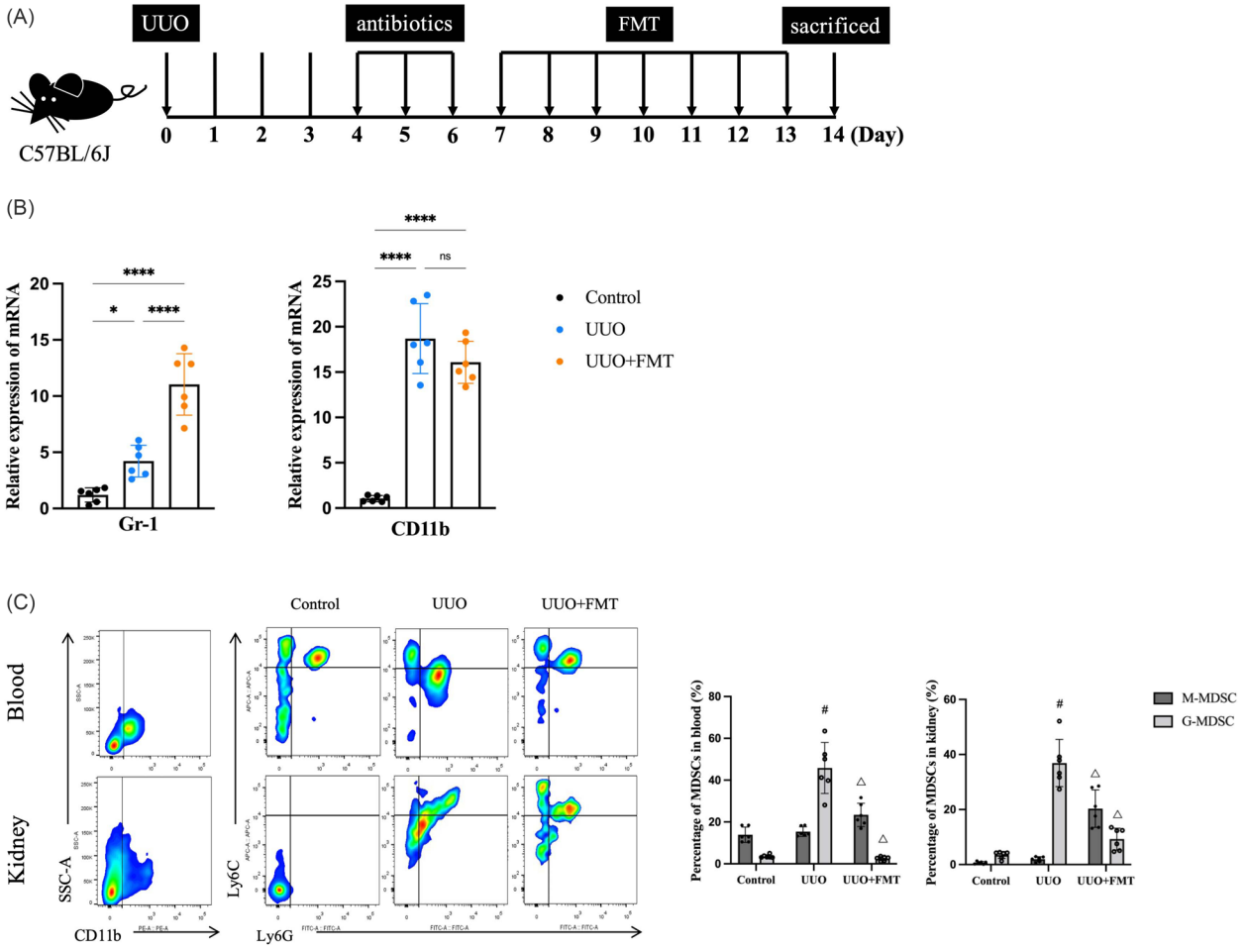


**Figure 1.** FMT regulated MDSCs mobilization after UUO. (A) Antibiotics were administered to mice on days 4, 5, and 6 after UUO, and then FMT treatment for 7 days. Kidneys, spleens and blood were extracted on day 14 after UUO. (B) Relative mRNA levels of Gr-1 and CD11b in renal tissue. *$p < 0.05$, ****$p < 0.0001$, ns^$p > 0.05$. (C) Flow cytometry detected the percentage of $CD11b^+$ $Ly6C^+$ M-MDSCs and $CD11b^+$ $Ly6G^+$ G-MDSCs in renal and blood. The ratio of M-MDSCs increased after FMT treatment, while the ratio of G-MDSCs decreased. Data are expressed as the mean ± SD ($n = 6$). #$p < 0.05$, vs. The control group, △$p < 0.05$ vs. The UUO group.

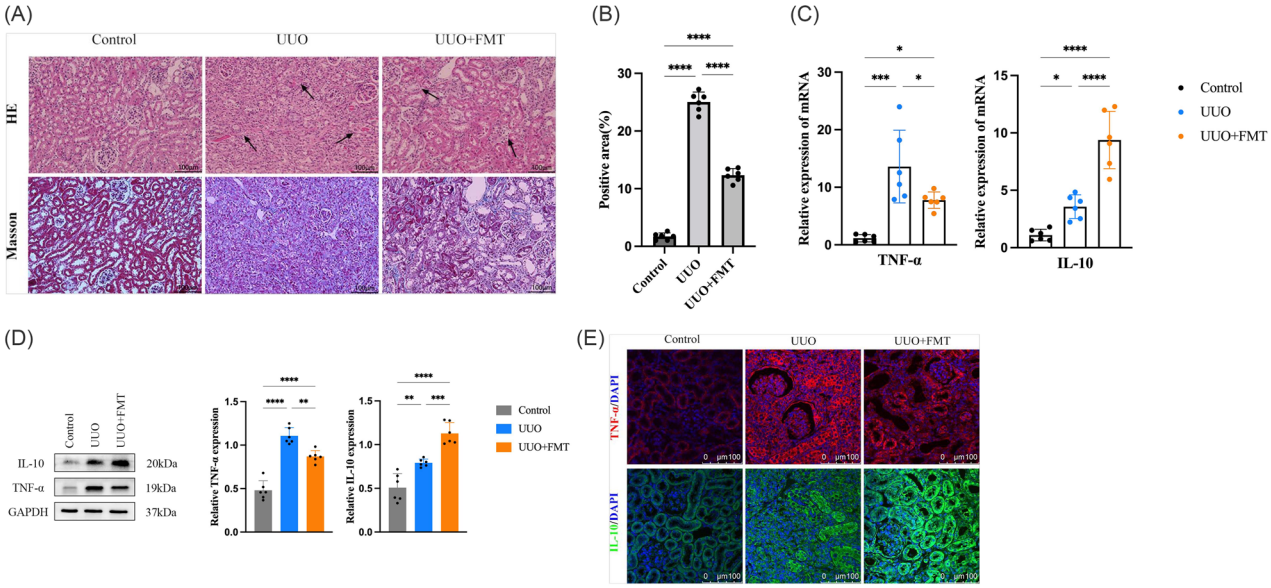


**Figure 2.** FMT protected against UUO injury. (A) HE and masson's trichrome staining were performed to describe and evaluate kidney injury. FMT treatment resulted in less kidney damage. (B) Collagen areas were quantified by masson's trichrome staining. (C) Relative mRNA levels of TNF-α and IL-10 in renal tissue. (D) The protein levels of TNF-α and IL-10 were assayed by Western blot and analyzed semi-quantitatively. (E) Representative immunofluorescence staining images of TNF-α (red), IL-10 (green), and DAPI (blue). The magnification of the images is ×200, scale bar = 100 μm. Data were presented as means ± SD ($n = 6$). *$p < 0.05$, **$p < 0.01$, ***$p < 0.001$, ****$p < 0.0001$.

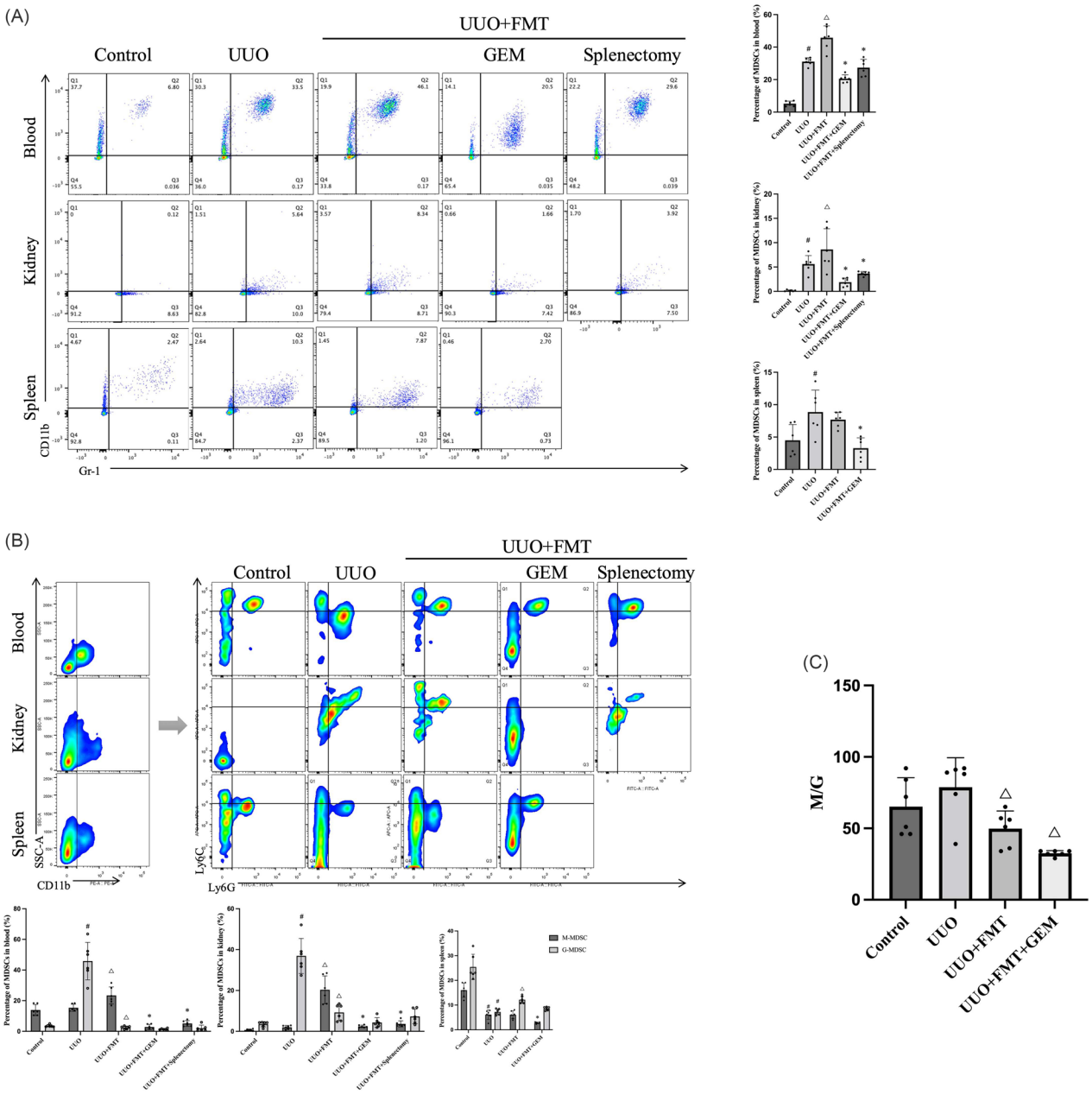


Figure 3. Regulation of MDSCs after gemcitabine treatment or splenectomy. Flow cytometry detected the percentages of $CD11b^+$ $Gr\text{-}1^+$ MDSCs (a), $CD11b^+$ $Ly6C^+$ M-MDSCs and $CD11b^+$ $Ly6G^+$ G-MDSCs (B) in blood, kidney and spleen. (C) Ratio of M-MDSC/G-MDSC in spleen. Data were presented as means ± SD ($n = 6$). $^{\#}p < 0.05$, vs. The control group, $\triangle p < 0.05$ vs. The UUO group, $^{*}p < 0.05$, vs. The UUO+FMT group.

indicating the occurrence of renal inflammation, and that FMT intervention ameliorated this abnormal TNF-α expression (Figure 2(D)). Moreover, IL-10 protein expression was greater in the UUO+FMT group than in the UUO group (Figure 2(D)). The same results were verified using immunofluorescence (Figure 2(E)). These findings confirmed the protective role of FMT in the kidneys of UUO model mice.

### *Regulation of MDSCs after gemcitabine treatment or splenectomy*

Gemcitabine has been shown to clear macrophages [23]. To investigate the potential role of spleen-derived MDSCs in FMT, we removed MDSCs by splenectomy or intraperitoneal injection of gemcitabine. MDSCs in the peripheral blood and kidneys were significantly reduced in the UUO+FMT+GEM and UUO+FMT+Splenectomy groups (Figure 3(A)). We demonstrated that gemcitabine treatment resulted in a reduction in the number of MDSCs in mouse spleens (Figure 3(A)). Moreover, the percentages of G-MDSCs and M-MDSCs were also altered, mainly due to the disappearance of M-MDSC dominance (Figure 3(B)). We also found that the M-MDSC/G-MDSC ratio in the spleen decreased after FMT (Figure 3(C)). Changes in the two types of MDSCs suggested a link between FMT treatment and MDSCs.

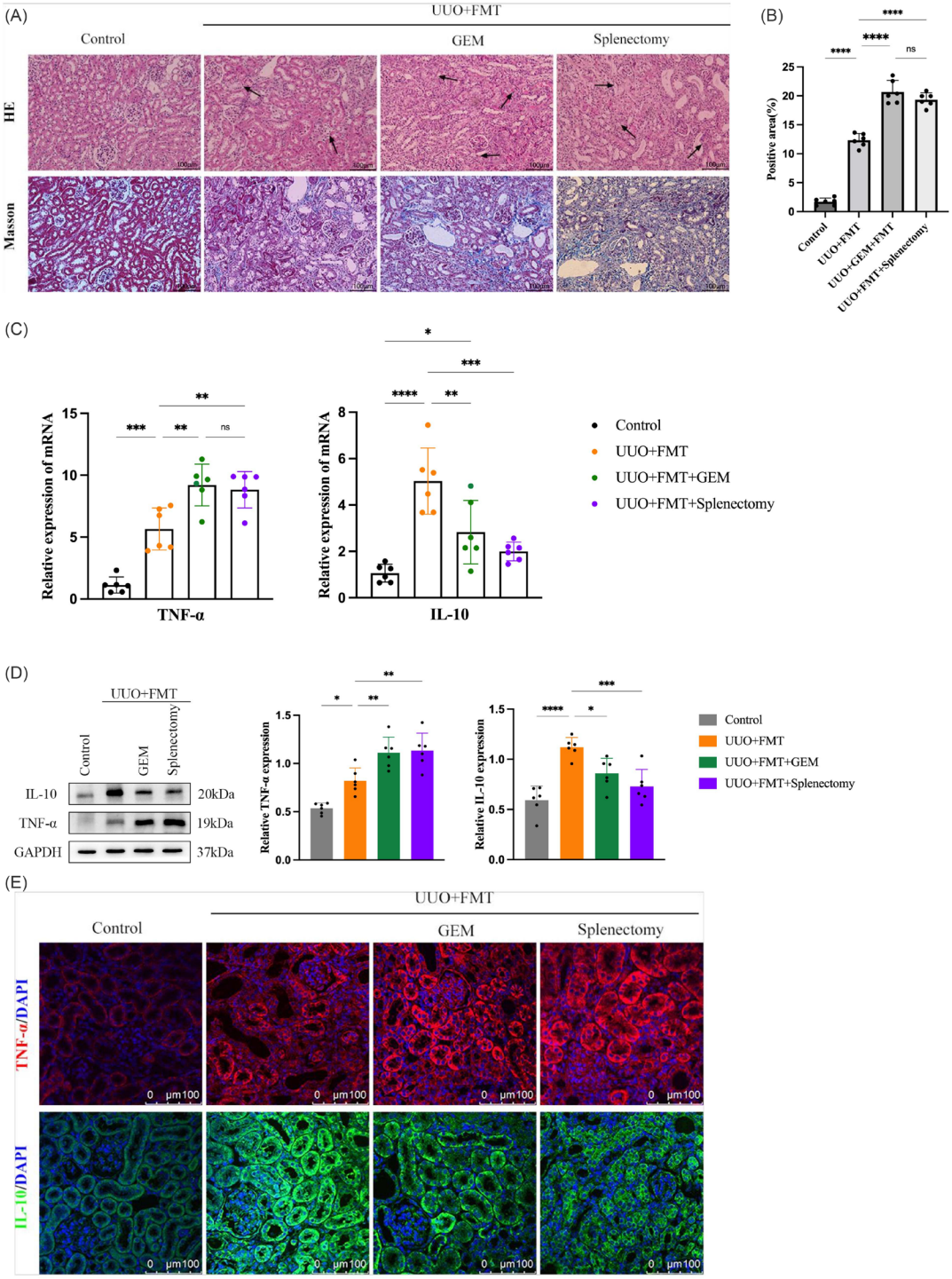


Figure 4. Eliminating MDSCs reduced the renal protection endowed by FMT. (A) HE and masson's trichrome staining were performed to describe and evaluate kidney injury. (B) Collagen areas were quantified by masson's trichrome staining. (C) Relative mRNA levels of TNF-α and IL-10 in renal tissue. (D) The protein levels of TNF-α and IL-10 were assayed by Western blot and analyzed semi-quantitatively. (E) Representative immunofluorescence staining images of TNF-α (red), IL-10 (green), and DAPI (blue). The magnification of the images is ×200, scale bar = 100 μm. Data were presented as means ± SD ($n = 6$). *$p < 0.05$, **$p < 0.01$, ***$p < 0.001$, ****$p < 0.0001$, ns^$p > 0.05$.

### *Eliminating MDSCs reduced the renal protection endowed by FMT*

To verify that FMT exerts its therapeutic effects through MDSCs, we examined renal injury and inflammation after removing MDSCs. HE and Masson's trichrome staining revealed greater renal injury and interstitial fibrosis in the UUO+FMT group after MDSC clearance than in the UUO+FMT group (Figure 4(A,B)). In addition, we found significant increases in TNF-α protein expression and decreases in IL-10 protein expression in the kidney tissues of the UUO+FMT+GEM group and the UUO+FMT+Splenectomy group (Figure 4(D)). There were no significant differences between the two

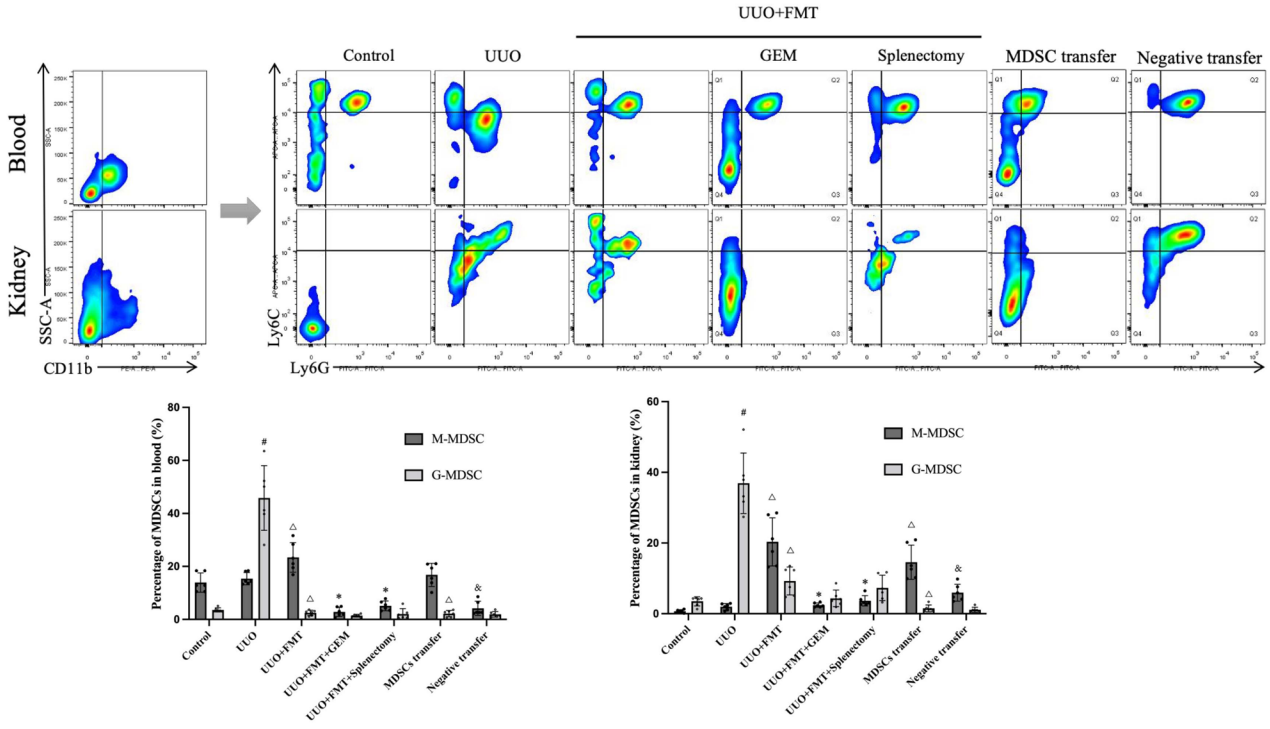


Figure 5. Flow cytometry detected the percentages of CD11b$^+$ Ly6C$^+$ M-MDSCs and CD11b$^+$ Ly6G$^+$ G-MDSCs in renal and blood. Data were presented as means ± SD ($n = 6$). $^{\#}p < 0.05$, vs. The control group, $\triangle p < 0.05$ vs. The UUO group, $^{*}p < 0.05$, vs. The UUO+FMT group, $^{\&}p < 0.05$ vs. The MDSCs transfer group.

groups. The same results were observed by qRT–PCR and immunofluorescence staining (Figure 4(C,E)). These results confirmed that the renoprotective effect of FMT treatment was reversed by the clearance of MDSCs.

### *Adoptively transferring MDSCs was beneficial in delaying renal fibrosis*

To further investigate the role of MDSCs in renal fibrosis, we adoptively transferred MDSCs dominated by M-MDSCs into renal fibrosis model mice. After the separation of MDSCs and negative control cells by magnetic columns, we determined the purity of the MDSCs to be approximately 78.6% by flow cytometry (Supplementary Figure). M-MDSCs were predominant in the peripheral blood and kidneys of mice in the MDSC group compared to the UUO group, while few MDSCs of both types were detected in the negative control group (Figure 5). We found that this treatment may be beneficial to the kidney. Renal tubular dilatation and renal fibrosis were ameliorated by the adoptive transfer of MDSCs (Figure 6(A,B)). Compared with that in the control group, the expression of proinflammatory factors increased significantly in the negative transfer group, while MDSC transfer reduced the expression of proinflammatory factors and promoted the expression of anti-inflammatory factors (Figure 6(C,D,E)). This evidence indicated a definite renoprotective effect of MDSC transplantation. M-MDSCs are most likely an anti-inflammatory type of MDSC in renal fibrosis.

## Discussion

In this study, we demonstrated that FMT ameliorated UUO-induced renal tubulointerstitial fibrosis and, for the first time, revealed the involvement of MDSCs in this nephroprotective process. We further elucidated that FMT induced changes in the number and ratio of the two subtypes of MDSCs, and more M-MDSCs were recruited to the kidney to exert anti-inflammatory and antifibrotic effects.

Most of the microorganisms that inhabit the human body reside in the gut, and the gut microbiota plays an important role in cultivating host immunity, regulating intestinal endocrine function, eliminating toxins, and producing a variety of compounds that affect the host [24]. Gut dysbiosis occurs at the onset of CKD and during the development of CKD and progression to end-stage kidney disease (ESKD) [4,25,26]. In a recent systematic review, compared to healthy controls, CKD patients had an increased abundance of the phyla Proteobacteria and Fusobacteria and a reduced presence of the genera Faecalibacterium, Roseburia, Pyramidobacter, Prevotella_9, and Prevotellaceae_UCG-001 [9]. Moreover, elevated levels of the bacterial metabolites trimethylamine n-oxide (TMAO) and p-cresol sulfate (PCS) and decreased production of short-chain fatty acids (SCFAs) were found in CKD patients [11]. The gut microbiota is also capable of manipulating the processes leading to CKD onset and progression through inflammatory, endocrine, and neurologic pathways [4]. The occurrence of intestinal dysbiosis after renal injury is well established. Mediating gut dysbiosis will be a new therapeutic direction for treating kidney disease.

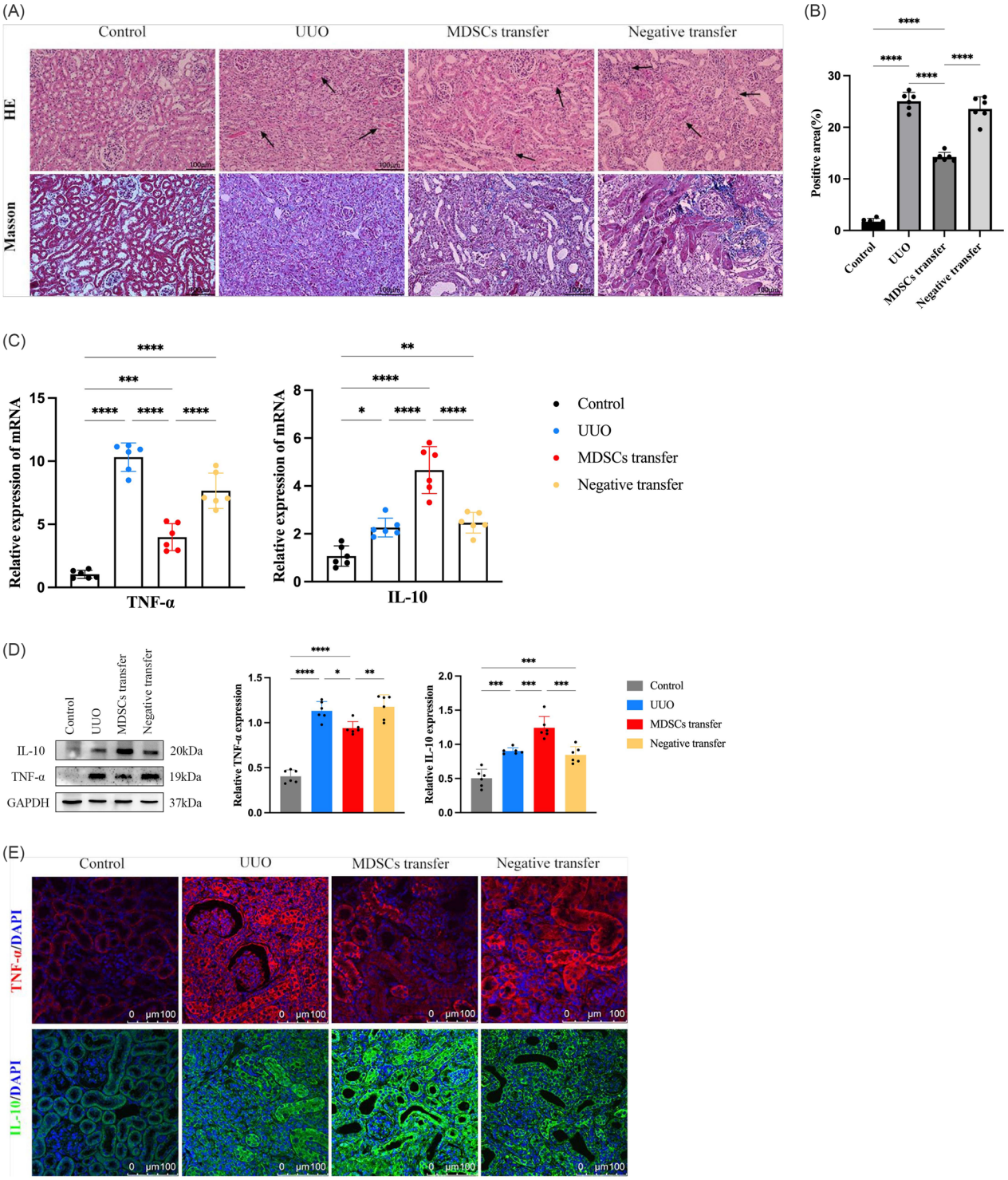


**Figure 6.** Adoptively transferring MDSCs benefited renal function. (A) HE and masson's trichrome staining were performed to describe and evaluate kidney injury. (B) Collagen areas were quantified by masson's trichrome staining. (C) Relative mRNA levels of TNF-α and IL-10 in renal tissue. (D) The protein levels of TNF-α and IL-10 were assayed by Western blot and analyzed semi-quantitatively. (E) Representative immunofluorescence staining images of TNF-α (red), IL-10 (green), and DAPI (blue). The magnification of the images is ×200, scale bar = 100 μm. Data were presented as means ± SD ($n = 6$). *$p < 0.05$, **$p < 0.01$, ***$p < 0.001$, ****$p < 0.0001$

FMT, as an emerging treatment, targets gut dysbiosis. Many studies have shown that FMT is beneficial for treating diseases associated with dysregulated gut microbiota, including obesity, type 2 diabetes, multiple sclerosis, and Alzheimer's disease [17,27,28,29]. Interestingly, Fernandes et al. reported that gut microbiota dysbiosis contributes to the development of kidney diseases through the release of inflammatory cytokines and uremic toxins [30]. For the first time, Hu et al. demonstrated that both gut microbiota depletion and FMT treatments alleviated tubulointerstitial injury in diabetic rats

[31]. In this study, we demonstrated a significant increase in the levels of inflammatory factors in renal fibrosis mice compared with those in control mice, but the level of the proinflammatory factor TNF-α was reduced in FMT-treated mice. Moreover, FMT treatment also alleviated tubulointerstitial injury in UUO model mice, which was characterized by ameliorated desquamation and necrosis of renal tubular epithelial cells and tubular deformation. However, the pathways through which FMT affects the kidney remain to be further studied.

Initially, MDSCs were described in cancer patients [32,33.34]. MDSCs have been shown to migrate to tumors due to the chemokine gradient generated by the growing tumor. The migration of MDSCs mainly relies on the expression of the chemokine receptor CXCR1/2 and its cognate ligands CXCL1, CXCL2 and CXCL5 [35]. Cysteine-rich intestinal protein 1 (CRIP1) binds to NF-κB/p65, leading to the transcriptional activation of CXCXL1/5, which promotes the chemotactic migration of MDSCs to drive immunosuppression [36]. MDSCs have recently received increasing attention for their functional importance in the immune system. The phenotype and activity of MDSCs depend largely on the environment in which they expand and function. We realized that MDSCs may be helpful to the host in certain circumstances but harmful in others. Previous studies have shown that MDSCs derived from early septic mice are proinflammatory, whereas MDSCs derived from late septic mice are immunosuppressive [37]. In our study, FMT-induced alterations in MDSCs were beneficial to mice with renal fibrosis. The total number of MDSCs and the number of both subtypes changed after FMT. Gemcitabine has been shown to reduce the number of MDSCs in the bone marrow and peripheral blood in addition to the percentage of MDSCs in the spleen [38]. After we removed MDSCs from mice by splenectomy or administration of gemcitabine, the renoprotective effects of FMT were abrogated. This suggested that functional MDSCs are likely derived primarily from the spleen.

G-MDSCs and M-MDSCs also have unique functional and biochemical characteristics. A previous study revealed that after renal ischemia–reperfusion injury, G-CSF treatment increased renal infiltration of MDSCs, especially G-MDSCs, to attenuate renal fibrosis [17]. Treatment with M-MDSC supernatant ameliorated renal fibrosis and myofibroblastic differentiation through IL-15 [39]. Other studies have suggested that M-MDSCs inhibit fibrosis in liver disease [40] and promote pulmonary fibrosis [41]. Our study showed that renal fibrosis mice treated with FMT had increased M-MDSCs and decreased G-MDSCs in the blood and kidneys. Since G-MDSCs were more prevalent in the spleen after FMT treatment, we speculated that perhaps M-MDSCs in the spleen were mobilized into the circulation and kidney to play a role. In addition, after the transfer of MDSCs dominated by M-MDSCs into renal fibrosis model mice, the levels of inflammatory factors decreased, reducing inflammation and renal fibrosis. These findings suggested that M-MDSCs may be an anti-inflammatory type of MDSC in renal fibrosis. We demonstrated that the anti-inflammatory activities of gut flora-induced MDSCs offer an alternative immunotherapy protocol for patients with chronic kidney disease.

Our study has several limitations. After FMT treatment, the expression of Gr-1 was elevated, while the change in CD11b expression was not statistically significant, which demonstrated that other immunocytes that can be labeled by CD11b may be involved during FMT intervention. The co-alteration of these cells with MDSCs led to the final result of CD11b expression. The immunomodulatory mechanisms involved in FMT should be further explored in the future. Second, the pathways and mechanisms involved in the effects of the two MDSC subtypes on renal inflammation and fibrosis have not been clarified. Third, considering that FMT affects multiple systems in the human body, its use as a therapeutic approach to alleviate renal fibrosis requires further optimization and validation.

## Conclusion

Fecal microbiota transplantation in UUO model mice can increase the proportion of M-MDSCs and inhibit the expression of proinflammatory cytokines, which provides a promising strategy for renal fibrosis treatment.

## Disclosure statement

No potential conflict of interest was reported by the author(s).

## Funding

This work was supported by Excellent Young Talents Fund Program of Higher Education Institutions of Anhui Province (Grant no.2023AH030107) and Talent Project of Anhui Provincial Department of Education (gxgwfx2021039, gxgwfx2020048).

## Data availability statement

All data produced or analyzed during this study are incorporated in this article or displayed in supplementary material.

## References

[1] Webster AC, Nagler EV, Morton RL, et al. Chronic kidney disease. Lancet. 2017;389(10075):1238–1252. doi: 10.1016/S0140-6736(16)32064-5.

[2] Humphreys BD. Mechanisms of renal fibrosis. Annu Rev Physiol. 2018;80(1):309–326. doi: 10.1146/annurev-physiol-022516-034227.

[3] Jandhyala SM, Talukdar R, Subramanyam C, et al. Role of the normal gut microbiota. World J Gastroenterol. 2015;21(29):8787–8803. doi: 10.3748/wjg.v21.i29.8787.

[4] Rukavina Mikusic NL, Kouyoumdzian NM, Choi MR. Gut microbiota and chronic kidney disease: evidences and mechanisms that mediate a new communication in the gastrointestinal-renal axis. Pflugers Arch. 2020;472(3):303–320. doi: 10.1007/s00424-020-02352-x.

[5] Yang T, Richards EM, Pepine CJ, et al. The gut microbiota and the brain-gut-kidney axis in hypertension and chronic kidney disease. Nat Rev Nephrol. 2018;14(7):442–456. doi: 10.1038/s41581-018-0018-2.
[6] Schluter J, Peled JU, Taylor BP, et al. The gut microbiota is associated with immune cell dynamics in humans. Nature. 2020;588(7837):303–307. doi: 10.1038/s41586-020-2971-8.
[7] Hu X, Xie Y, Xiao Y, et al. Longitudinal analysis of fecal microbiome and metabolome during renal fibrotic progression in a unilateral ureteral obstruction animal model. Eur J Pharmacol. 2020;886:173555. doi: 10.1016/j.ejphar.2020.173555.
[8] Zhou W, Wu WH, Si ZL, et al. The gut microbe Bacteroides fragilis ameliorates renal fibrosis in mice. Nat Commun. 2022;13(1):6081. doi: 10.1038/s41467-022-33824-6.
[9] Bian J, Liebert A, Bicknell B, et al. Faecal microbiota transplantation and chronic kidney disease. Nutrients. 2022;14(12):2528. doi: 10.3390/nu14122528.
[10] Mishima E, Fukuda S, Mukawa C, et al. Evaluation of the impact of gut microbiota on uremic solute accumulation by a CE-TOFMS-based metabolomics approach. Kidney Int. 2017;92(3):634–645. doi: 10.1016/j.kint.2017.02.011.
[11] Zhao J, Ning X, Liu B, et al. Specific alterations in gut microbiota in patients with chronic kidney disease: an updated systematic review. Ren Fail. 2021;43(1):102–112. doi: 10.1080/0886022X.2020.1864404.
[12] Cammarota G, Ianiro G, Tilg H, et al. European consensus conference on faecal microbiota transplantation in clinical practice. Gut. 2017;66(4):569–580. doi: 10.1136/gutjnl-2016-313017.
[13] Barba C, Soulage CO, Caggiano G, et al. Effects of fecal microbiota transplantation on composition in mice with CKD. Toxins (Basel). 2020;12(12):741. doi: 10.3390/toxins12120741.
[14] Gabrilovich DI, Nagaraj S. Myeloid-derived suppressor cells as regulators of the immune system. Nat Rev Immunol. 2009;9(3):162–174. doi: 10.1038/nri2506.
[15] Bronte V, Brandau S, Chen SH, et al. Recommendations for myeloid-derived suppressor cell nomenclature and characterization standards. Nat Commun. 2016;7(1):12150. doi: 10.1038/ncomms12150.
[16] Qiu Y, Cao Y, Tu G, et al. Myeloid-derived suppressor cells alleviate renal fibrosis progression via regulation of CCL5-CCR5 axis. Front Immunol. 2021;12:804228. doi: 10.3389/fimmu.2021.698894.
[17] Yan JJ, Ryu JH, Piao H, et al. Granulocyte colony-stimulating factor attenuates renal ischemia-reperfusion injury by inducing myeloid-derived suppressor cells. J Am Soc Nephrol. 2020;31(4):731–746. doi: 10.1681/ASN.2019060601.
[18] Hsu CY, Lin YC, Chang LY, et al. Therapeutic role of inducible nitric oxide synthase expressing myeloid-derived suppressor cells in acetaminophen-induced murine liver failure. Front Immunol. 2020;11:574839. doi: 10.3389/fimmu.2020.574839.
[19] Yang CJ, Peng YS, Sung PC, et al. Protocol for oral fecal gavage to reshape the gut microbiota in mice. STAR Protoc. 2025;6(1):103585. doi: 10.1016/j.xpro.2024.103585.
[20] Zhao S, Zhang H, Zhu H, et al. Gut microbiota promotes macrophage M1 polarization in hepatic sinusoidal obstruction syndrome via regulating intestinal barrier function mediated by butyrate. Gut Microbes. 2024;16(1):2377567. doi: 10.1080/19490976.2024.2377567.
[21] Sun J, Xu J, Ling Y, et al. Fecal microbiota transplantation alleviated Alzheimer's disease-like pathogenesis in APP/PS1 transgenic mice. Transl Psychiatry. 2019;9(1):189. doi: 10.1038/s41398-019-0525-3.
[22] Li SC, Rangel AD, Kabeer MH. Precision technique for splenectomy limits mouse stress responses for accurate and realistic measurements for investigating inflammation and immunity. Bio Protoc. 2019;9(15):e3317. doi: 10.21769/BioProtoc.3317.
[23] Suzuki E, Kapoor V, Jassar AS, et al. Gemcitabine selectively eliminates splenic Gr-1+/CD11b+myeloid suppressor cells in tumor-bearing animals and enhances antitumor immune activity. Clin Cancer Res. 2005;11(18):6713–6721. doi: 10.1158/1078-0432.CCR-05-0883.
[24] Lynch SV, Pedersen O. The human intestinal microbiome in health and disease. N Engl J Med. 2016;375(24):2369–2379. doi: 10.1056/NEJMra1600266.
[25] Hu X, Ouyang S, Xie Y, et al. Characterizing the gut microbiota in patients with chronic kidney disease. Postgrad Med. 2020;132(6):495–505. doi: 10.1080/00325481.2020.1744335.
[26] Mafra D, Kalantar-Zadeh K, Moore LW. New tricks for old friends: treating gut microbiota of patients with CKD. J Ren Nutr. 2021;31(5):433–437. doi: 10.1053/j.jrn.2021.07.002.
[27] Li K, Wei S, Hu L, et al. Protection of fecal microbiota transplantation in a mouse model of multiple sclerosis. Mediators Inflamm.2020;2020:2058272. doi: 10.1155/2020/2058272.
[28] Ng SC, Xu Z, Mak JWY, et al. Microbiota engraftment after faecal microbiota transplantation in obese subjects with type 2 diabetes: a 24-week, double-blind, randomised controlled trial. Gut. 2022;71(4):716–723. doi: 10.1136/gutjnl-2020-323617.
[29] Yu EW, Gao L, Stastka P, et al. Fecal microbiota transplantation for the improvement of metabolism in obesity: the FMT-TRIM double-blind placebo-controlled pilot trial. PLoS Med. 2020;17(3):e1003051. doi: 10.1371/journal.pmed.1003051.
[30] Fernandes R, Viana SD, Nunes S, et al. Diabetic gut microbiota dysbiosis as an inflammaging and immunosenescence condition that fosters progression of retinopathy and nephropathy. Biochim Biophys Acta Mol Basis Dis. 2019;1865(7):1876–1897. doi: 10.1016/j.bbadis.2018.09.032.
[31] Hu ZB, Lu J, Chen PP, et al. Dysbiosis of intestinal microbiota mediates tubulointerstitial injury in diabetic nephropathy via the disruption of cholesterol homeostasis. Theranostics. 2020;10(6):2803–2816. doi: 10.7150/thno.40571.
[32] Buessow SC, Paul RD, Lopez DM. Influence of mammary tumor progression on phenotype and function of spleen and in situ lymphocytes in mice. J Natl Cancer Inst. 1984;73(1):249–255.
[33] Seung LP, Rowley DA, Dubey P, et al. Synergy between T-cell immunity and inhibition of paracrine stimulation causes tumor rejection. Proc Natl Acad Sci U S A. 1995;92(14):6254–6258. doi: 10.1073/pnas.92.14.6254.
[34] Young MR, Newby M, Wepsic HT. Hematopoiesis and suppressor bone marrow cells in mice bearing large metastatic Lewis lung carcinoma tumors. Cancer Res. 1987;47:100–105.
[35] Nagarsheth N, Wicha MS, Zou W. Chemokines in the cancer microenvironment and their relevance in cancer

immunotherapy. Nat Rev Immunol. 2017;17(9):559–572. doi: 10.1038/nri.2017.49.

[36] Liu X, Tang R, Xu J, et al. CRIP1 fosters MDSC trafficking and resets tumour microenvironment via facilitating NF-κB/p65 nuclear translocation in pancreatic ductal adenocarcinoma. Gut. 2023;72(12):2329–2343. doi: 10.1136/gutjnl-2022-329349.

[37] Dai J, El Gazzar M, Li GY, et al. Myeloid-derived suppressor cells: paradoxical roles in infection and immunity. J Innate Immun. 2015;7(2):116–126. doi: 10.1159/000368233.

[38] Le HK, Graham L, Cha E, et al. Gemcitabine directly inhibits myeloid derived suppressor cells in BALB/c mice bearing 4T1 mammary carcinoma and augments expansion of T cells from tumor-bearing mice. Int Immunopharmacol. 2009;9(7-8):900–909. doi: 10.1016/j.intimp.2009.03.015.

[39] Cheuk YC, Xu S, Zhu D, et al. Monocytic myeloid-derived suppressor cells inhibit myofibroblastic differentiation in mesenchymal stem cells through IL-15 secretion. Front Cell Dev Biol. 2022;10:817402. doi: 10.3389/fcell.2022.817402.

[40] Wang Y, Guo X, Jiao G, et al. Splenectomy promotes macrophage polarization in a mouse model of concanavalin A- (ConA-) induced liver fibrosis. Biomed Res Int. 2019;2019:5756189. doi: 10.1155/2019/5756189.

[41] Fu C, Lu Y, Williams MA, et al. Emergency myelopoiesis contributes to immune cell exhaustion and pulmonary vascular remodelling. Br J Pharmacol. 2021;178(1):187–202. doi: 10.1111/bph.14945.